





# Combining geophysical and geomorphological data to reconstruct the development of relief of a medieval castle site in the Spessart low mountain range, Germany

Julian Trappe  | Christian Büdel  | Julia Meister  | Roland Baumhauer 

Chair of Physical Geography, Institute of Geography and Geology, University of Würzburg, Würzburg, Germany

## Correspondence

Julian Trappe, Chair of Physical Geography, Institute of Geography and Geology, University of Würzburg, Würzburg, Germany.  
Email: julian.trappe@uni-wuerzburg.de

## Abstract

Within the Spessart low mountain range in central Germany, numerous castle ruins of the 13th century CE exist. Their construction and destruction were often determined by the struggle for political and economic supremacy in the region and for control over the Spessart's natural resources. Wahlmich Castle is located in a relatively uncommon strategic and geomorphological position, characterized by a fairly remote position and atypical rough relief. In order to reconstruct the local relief development and possible human impact, a multi-method approach was applied combining two-dimensional geoelectrical measurements, geomorphological mapping and stratigraphic-sedimentological investigations. This provides new insights into the influence of landscape characteristics on choices of castle locations.

The combined geoelectrical, geomorphological and stratigraphic-sedimentological data show that the rough relief is of natural origin and influenced by regional faulting, which triggered sliding and slumping as well as weathering and dissection of the surface deposits. The rough relief and the lithology permitted intensive land use and building activities. However, the location of the castle offered access to and possibly control over important medieval traffic routes and also represented certain ownership claims in the Aschaff River valley.

The economic situation combined with rivalry between different elites led to the castle being built in a geomorphological challenging and strategically less valuable location. Focusing on castles located in rare and challenging geomorphological positions may therefore lead to a better understanding of castle siting in the future.

## KEYWORDS

faulting, geoarchaeology, geomorphological mapping, geophysical prospection, percussion core probing, sedimentology

## 1 | INTRODUCTION

The location of medieval castles at prominent points in a larger landscape was often dictated by the requirements of military strategy and a desire to represent authority. In addition, the specific natural environment and its suitability in functional and structural terms, such as the distance to roads and settlements or the availability of water and security, determined the individual type and nature of a castle

(cf., Kolb & Krenig, 1989; Ruf, 1984, 2019; Schäfer, 2000; Schecher, 1969). Within the Spessart – a low mountain range in central Germany (Figure 1) – there are numerous castle ruins of the 13th century CE (e.g., Gröber & Karlinger, 1916; Ruf, 2019). Several of these castles were constructed and destroyed during the territorial feud between the Counts of Rieneck and the Bishops of Mainz. The distribution of castles within the Spessart was generally related to population density, the economics of the medieval communities, and political

This is an open access article under the terms of the Creative Commons Attribution License, which permits use, distribution and reproduction in any medium, provided the original work is properly cited.

© 2021 The Authors. *Earth Surface Processes and Landforms* published by John Wiley & Sons Ltd.

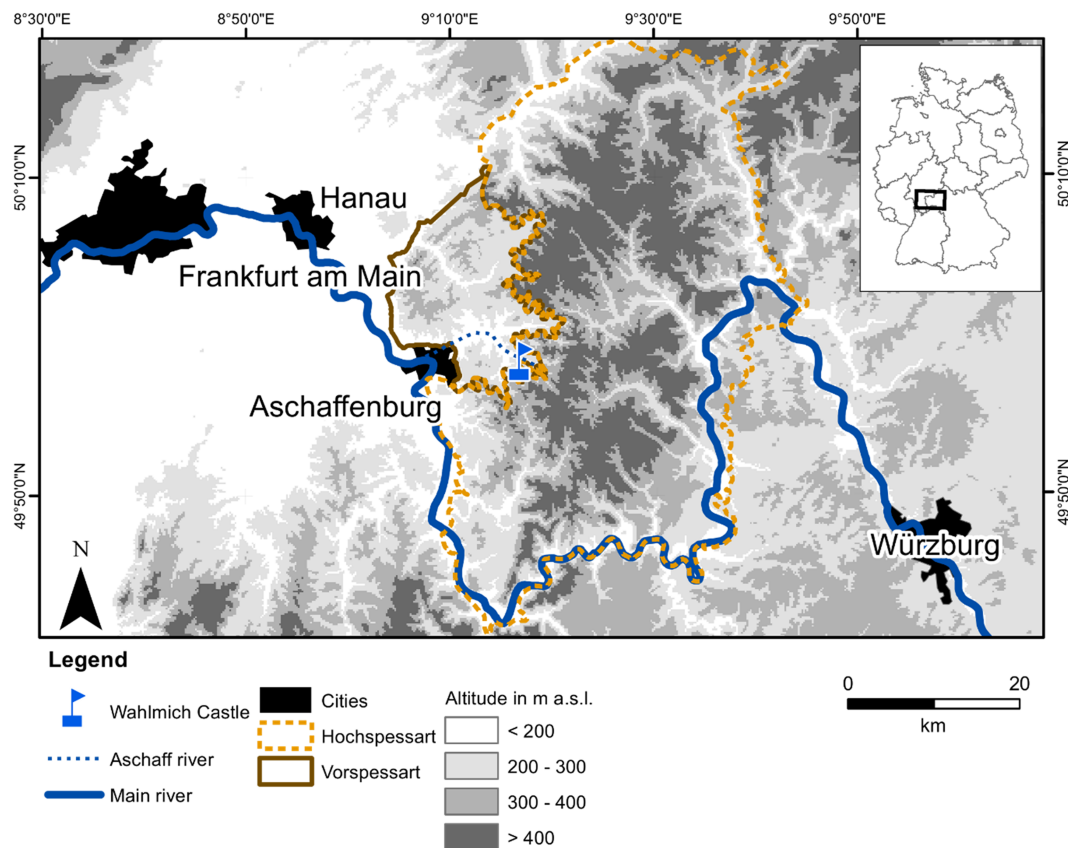


**FIGURE 1** Location of the Spessart within Germany and the case study site Wahlmich Castle. Basemap: DEM from: ASTER DEM (ASTGTMv003 2019) [Color figure can be viewed at [wileyonlinelibrary.com](https://onlinelibrary.wiley.com)]

decisions. All these factors are usually well known and discussed in historical and archaeological studies (cf., Kemethmüller, 2011; Rosmanitz, 2011; Ruf, 2019).

However, a comparison between the distribution of castle sites in the Spessart and the geomorphological setting reveals certain patterns as well. In the western Spessart, for example, a concentration of castles at a considerable distance from the Mesozoic Cuesta escarpment is evident (Figure 2). Furthermore, there is a preference for castle sites along the Main River valley, while central and eastern Spessart harbours far fewer castle sites. Isolated inselbergs, however, are classic locations for military fortifications and therefore usually occupied by large castles.

To identify general locational factors and assess their significance, geoscientific evidence and historical and archaeological records of several castle sites should be compared. To examine the relationship of an individual medieval castle to its adjacent landscape, a more detailed spatial scale is required. The question arises as to the extent to which natural resources and ecosystem services determined castle siting.

In this context, Wahlmich Castle offers an ideal opportunity to gain new insights into the influence of landscape characteristics on the choice of a castle location in a clear and well-defined space by using a geoscientific multi-method approach. Situated in the Cuesta escarpment, Wahlmich Castle is located in a relatively unusual and almost unique strategic and geomorphological position, characterized by atypical rough relief. The objectives of this study are therefore (i) to investigate whether this particular relief is a natural feature of

the Cuesta landscape or whether it was created by medieval building activity, and (ii) in doing so, to examine a possible influence of morphological characteristics on the choice of the castle location.

## 2 | STUDY SITE

### 2.1 | Regional setting

The Spessart low mountain range is located in central Germany and can be divided along an articulated cuesta scarp into the Vorspessart in the west and the Hochspessart in the east (Figure 2). The largely uncovered bedrock of the Vorspessart comprises widely crystalline, Palaeozoic rocks mainly made of gneiss, quartzite and mica schist, whereas the crystalline rocks of the Hochspessart are mostly covered by Early Triassic rocks of Buntsandstein (or Bunter sandstone), which consists of sandstone with few conglomerates and claystone layers (e.g., Okrusch et al., 2011).

Wahlmich Castle is located in the Vorspessart, where the crystalline bedrock complex is made of Devonian Diorite and Granodiorite, classified according to its varying contents of orthoclase (Okrusch et al., 2011; Weinelt, 1962). For simplification, the Diorite–Granodiorite complex is referred to as ‘Grano-)Diorite’ in the following. Within the study area, a thin layer of the so-called ‘Brückelschiefer’ occasionally covers the crystalline bedrock. The sedimentary rock of the Brückelschiefer formation consists mainly of red claystone with intercalated grey clay, silt and sandstone, reaching a

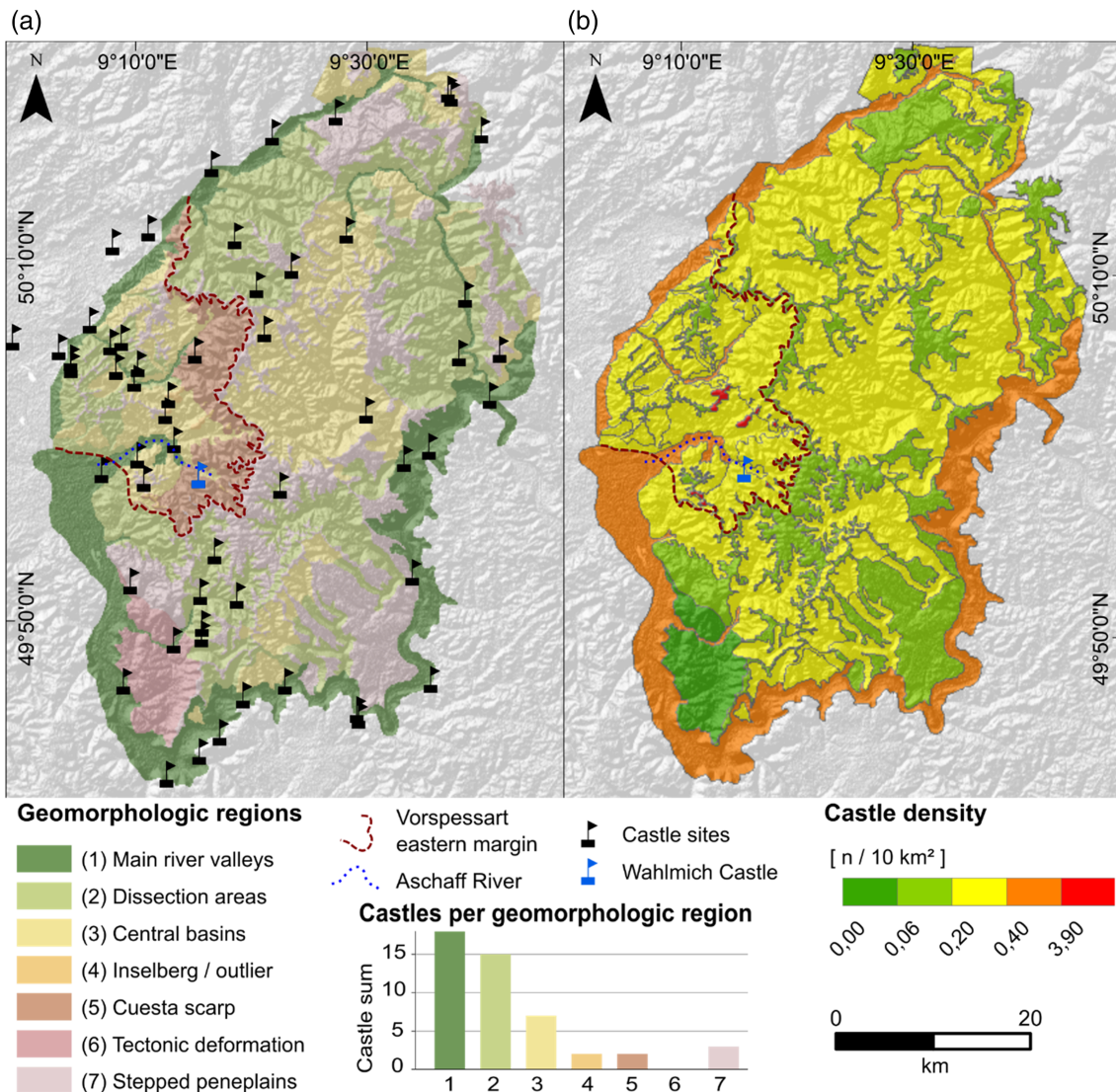


**FIGURE 2** Medieval castle distribution (a) and geomorphology of the Spessart low mountain range. Geomorphological regions represent simplified geomorphological regions derived from the detailed geomorphological classification provided by Jung (2006). Castle density (b) describes the number ( $n$ ) of castles per 10 km<sup>2</sup>; base map: hillshade from the ASTER DEM (ASTGTMv003 2019) [Color figure can be viewed at [wileyonlinelibrary.com](http://wileyonlinelibrary.com)]

maximum thickness of about 20 m. The Bröckelschiefer is part of the local Fulda-sequence, the last sequence of the Lopingian that forms part of the upper Permian (Käding, 1978). The bottom layer of the Bröckelschiefer, the so-called ‘Basalbrekzie’ (or basal-breccia; Okrusch et al., 2011), is defined as a mixed layer of Bröckelschiefer and the underlying material, in the case of this study the (Grano-) Diorite, which has no clear upper boundary (Scheinpflug, 1992).

Tectonic activity is indicated by several faults, which strike predominantly northwest–southeast (NW–SE), following the general Hercynian trend that was active mainly in the Tertiary (Jung, 2006; Murawski, 1965; Weinelt, 1962). In addition, a north–northwest–south–southwest (NNE–SSW)-striking Rhenish trend exists that has been active since the Tertiary (Meschede, 2019) and defines the anticlinal structures of the crystalline basement of the Spessart (Okrusch et al., 2011).

Quaternary deposits of shallow depth occasionally cover the sedimentary and crystalline bedrock. These are mainly associated with Periglacial Cover Beds (PCBs), which developed during glacial periods of the Pleistocene and typically include structures like solifluction

features, melt water channel accumulations and ice wedges (Meschede, 2019; Shishkina et al., 2019). The diagnostic properties of PCBs are specific structures of different movement processes, sorting characteristics and varying lithologic components and origins. Typically, three to four significant layers can be distinguished in the field (Ad-hoc Boden, 2005; Kleber, 1997; Kleber & Terhorst, 2013). PCBs of the crystalline Vorspessart area were studied and precisely described during the last years by Mueller (2011) and Mueller and Thiemeyer (2014). Soils in this area are classified as Cambisols and Regosols (Bayerisches Landesamt für Umwelt, 2015). Climatically, the Spessart is characterized by a Cfb-climate after Köppen and Geiger with average temperatures around 10°C and an annual precipitation of about 700 mm/a (Bayerisches Landesamt für Landwirtschaft, 2019).

During the Middle Ages, the resources of the Spessart were of high economic importance and an extensive trade network connected the centrally located Spessart region with important European trading cities such as Venice, Nuremberg, Frankfurt, Leipzig and Antwerp (Himmelsbach, 2005, 2014; Kampfmann & Krimm, 1988;

Landau, 1958). Of particular importance were the rich stands of European beech (*Fagus sylvatica*) (Büdel et al., 2021; Lagies, 2005; Zerbe, 1997), which in combination with high water availability were an important prerequisite for highly profitable glass production (Ermischer, 2019; Wedepohl, 2003). Organized glass production thus commenced comparatively early in the Spessart region, in the 11th century CE (Wamser, 1979, 1982). Extensive mining activities and ore extraction have only been documented in the Spessart region since the 15th century CE (Freyman, 1991), however, there is some archaeological evidence of earlier iron ore extraction and processing (Hasenstein et al., 2019; Lorenz et al., 2010).

## 2.2 | Wahlmich Castle

The castle ruin 'Wahlmich' close to the village of Waldaschaff has been excavated and investigated since 2016. Wahlmich Castle was constructed around 1220 CE as a stone fortification with a few workshops and farm buildings on top of a small isolated hard rock hill surrounded by neck trenches in a hillside position (Rosmanitz & Bachmann, 2017). The castle was destroyed as early as the late 1260s CE, sometime after the defeat of the Counts of Rieneck in March 1266, who had contractually agreed to the destruction of their castle on Mainz territory (Rosmanitz & Bachmann, 2017; Rosmanitz et al., 2019a, 2019b).

Wahlmich Castle is located within the Aschaff River valley, a tributary of the Main River, and has a distinct geomorphological setting (Figure 3a and Figure 4). The site is situated in a midslope to footslope position and the slope declines in elevation toward the north. The uphill area to the south generally features a gentle, continuous slope, while the immediate surrounding area to the south of the castle hill is characterized by several slope steps, scars, small ridges and valleys (Figure 4a,b). This rough terrain is very different from the surrounding landscape, which raises the question of whether the area has been shaped by human activity. However, apart from the castle itself, where artificial trenches and other earthworks, such as the gate ramp and the basement of the curtain wall, alter the topography of the castle hill, there is no obvious indication of intensive anthropogenic land use or evidence of building activities (Rosmanitz & Bachmann, 2017). Today, the castle hill and its direct surroundings are mainly covered by beech forests; a few 100 m south and east of the castle keep, meadows occur (Figure 3b,c).

## 3 | METHODS

To investigate landscape development and human activity in the surroundings of Wahlmich Castle, a multi-method approach was applied, combining sedimentological and geomorphological studies with electrical resistivity tomography (ERT) measurements. In addition to core drillings, geographic information system (GIS)-based geomorphological mapping and terrain analyses were carried out that are commonly applied for site descriptions and the morphometric delineation and description of landforms (e.g., Siart et al., 2018). Based on the available geological and archaeological records of the study area (Rosmanitz & Bachmann, 2017; Weinelt, 1962), the expected different lithological units should be detectable by differences in subsurface

electrical resistivities using ERT measurements (e.g., Telford et al., 1990) and well interpretable in combination with stratigraphic studies. Overall, a combination of geomorphological mapping and ERT is used frequently in geomorphological and tectonic investigations (Bernatek-Jakiel & Kondracka, 2016), while a combination of ERT and stratigraphic-sedimentological investigations is common in geomorphological studies (e.g., Kaufmann & Romanov, 2017; Sass et al., 2008; Trappe & Kneisel, 2019) and in the context of archaeological excavations (Fischer et al., 2016; Lange-Athinodorou et al., 2019; Siart et al., 2010).

### 3.1 | Stratigraphic-sedimentological fieldwork

The stratigraphic-sedimentological fieldwork included the description of soils and sediments from soil prospection pits and coring sites. Percussion core probing was conducted using a Wacker Neuson BH65 demolition hammer with drilling diameters from 30 to 80 mm. Sediment description followed the German guidelines for soil description (Ad-hoc Boden, 2005). This included the identification of PCBs and the evaluation of their preservation, which depends on the intensity soil development and the occurrence and thickness of the specific layers (Mueller & Thiemeyer, 2014). Rock units were identified according to their characteristics as given in Okrusch et al. (2011).

### 3.2 | Geomorphological mapping

All mapping was performed in a GIS using standard tools of ArcGIS (Esri) and SAGA GIS (©Conrad2002–2020). Land surface parameters (LSPs) were calculated from a LiDAR (light detection and ranging)-based digital elevation model (DEM) with a spatial resolution of 1 m pixel size (source: Bayerisches Landesamt für Digitalisierung, Breitband und Vermessung, 2014), including raster layers for slope, curvature and exposition, as well as a standard hillshade. Semi-automated landform classifications were derived by applying the topographic positioning index (TPI), which measures the relative topographic position of a focal point as the difference between the elevation at this point and the mean elevation within a predetermined neighbourhood (Weiss, 2001). A multi-scale TPI image was generated with estimation window sizes of 25 m and 150 m in diameter using the SAGA GIS multi-scale TPI tool (Guisan et al., 1999).

The identification and description of landforms followed the modified rules of the detailed geomorphological mapping system for geomorphological maps of the Federal Republic of Germany at the scale of 1:25,000 (GMK 5; Leser & Stäblein, 1985). Subsequently, the landforms were affiliated to six levels, assigned as 'level of incision' (Champagnac et al., 2014; Shishkina et al., 2019). This expert-based classification delineates and classifies all land surfaces according to the form, slope and direction of their drainageways and enclosing relief levels and slope shoulders. The approach is based on the observation that slope erosion is directly triggered by accelerated incision into drainageways and gullies. Incision occurs not only in a vertical direction, but also in varying spatial patterns and densities. Both properties are directly related to the processes occurring on the accompanying hillslopes. Thus, the intensity of the slope processes can be

quantified indirectly by means of the morphometric parameters of the mapped landforms. The level of incision therefore reflects the relief evolution of a defined area or set of landforms and semi-quantitatively describes the rates of erosion and their spatial distribution. The higher the level of incision, the higher the rate of incision and erosion.

### 3.3 | Electrical resistivity tomography (ERT)

ERT measurements were conducted along five profiles in the surroundings of the castle keep in order to obtain information on the subsurface structure (Figure 5f). Measurements were carried out using a Syscal Junior Switch (IRIS Instrument S.A.S.; Orléans, France) and a Wenner–Schlumberger electrode array, due to a good signal-to-noise ratio (e.g., Dahlin & Zhou, 2004). All data points with a deviation of 5% or more between individual, reciprocal measurements were deleted in order to enhance data quality. ERT data were inverted using the Res2dinv (Geotomosoft; Penang, Malaysia) software package and applying the fifth iteration of the robust inversion (L1-norm) scheme. While the ERT profiles E1 and E3 were measured with 72 electrodes, 936 quadripoles and an electrode spacing of 1.5 and 2 m, ERT profiles E2, E4 and E5 were measured with 36 electrodes, 288 quadripoles and electrode spacing of 2 and 3 m (Table 1). Whenever previous investigations suggested small-scale lithological changes and a shallow depth of cover deposits, a smaller spacing was chosen, while where thick cover layers were expected, a wider spacing was used.

To ensure the overall comparability of ERT depth sections, data from different profiles were displayed using the same legend categories for electrical resistivity, given in ohm-metre ( $\Omega\text{m}$ ) (Figure 5).

### 3.4 | Positioning

Due to different vegetation densities, different positioning techniques were used. The positions and absolute elevations of the single electrodes of ERT transects E3, E4 and E5 and core sites C5, C6, C7, C8 and C9 were measured using a Leica Multistation Tachymeter (Leica Camera AG; Wetzlar, Germany) that was positioned with fixed points of the archaeological excavation. The locations of the electrodes of ERT profiles E1 and E2 and core sites C1, C2, C3 and C4 were measured by means of a differential global positioning system (GPS; Leica GS15) with real-time kinematic of SAPOS with a precision  $\leq 5$  cm.

**TABLE 1** Name, spacing, number of electrodes and total length of the electrical resistivity tomography (ERT) profiles

Name	Spacing (m)	Number of electrodes	Total length (m)
E1	2	72	142
E2	2	36	70
E3	1.5	72	106.5
E4	3	36	105
E5	3	36	105

## 4 | RESULTS

### 4.1 | Stratigraphical overview

In the rough terrain south of the castle keep, nine sediment cores were drilled to a maximum depth of 11 m below ground surface. In addition, two outcrops were investigated (for core and outcrop locations see Figure 3a).

As expected from the preliminary geological and pedological work in the area, different lithological units were observed and simplified to (i) PCBs, (ii) Bröckelschiefer and (iii) (Grano-)Diorite (Figure 3d–i). Usually the basal unit is made of (Grano-)Diorite, overlain by a layer of Bröckelschiefer of varying thickness, which is covered by a PCB of a varying degree of preservation. (Grano-)Diorite and Bröckelschiefer saprolite thereby occur in various degrees of weathering (Figure 3i). At the bottom of the Bröckelschiefer formation, the basal-breccia is located. Here the amount of relatively unweathered (Grano-)Diorite fragments often increases and marks the transition from Bröckelschiefer to (Grano-)Diorite; it therefore served as initial stratigraphical evidence for the (Grano-)Diorite, although it is genetically part of the Bröckelschiefer.

The internal structure of the Bröckelschiefer facies varies considerably within the study area. In some areas, the red claystone is little weathered and shows the characteristic bedding of intercalated claystone and silty clay. In other areas, the claystone is intensely weathered and embedded in a red silty clay matrix with no visible layering. Moreover, the red clay matrix accommodates clay packages and sand or silt lenses and layers, independent of its weathering state. Even within a sedimentary profile, the Bröckelschiefer often occurs in several forms: the lower layers are mostly characterized by solid Bröckelschiefer but loose, undifferentiated Bröckelschiefer is frequently found in the upper layers.

The PCBs are mainly developed within the unconsolidated Bröckelschiefer, showing evidence of sliding or flowing movements that altered the structure of the rocks and could be clearly distinguished from the consolidated Bröckelschiefer through macroscopic marks of compaction and contorted layers (Figure 3d,g,h). On the slopes to the south and southeast of the castle site, the PCBs are well preserved, so that a clear distinction between the basal and upper layers is possible. However, the preservation decreases with increasing proximity to the castle hill, where the upper layers are often eroded and the basal layers are only rarely detectable. Overall, no evidence of anthropogenic construction activity and land use was found in the vicinity of the castle.

### 4.2 | Geomorphological landforms, levels of incision and stratigraphy

The analysis of the DEM and the classification of the local geomorphology revealed the dominant landforms of the study site, such as terrain levels, ridges, depressions and drainageways. Elevated landforms are clearly distinguishable from low elevated positions by their TPI values; ridges and terrain steps are characterized by high TPI values, while depressions and drainage basins are characterized by low TPI values (Figure 4a).

The actual extent of the former castle is still unknown and largely hidden, while the former keep is clearly visible due to the destroyed walls and could be mapped accordingly. With regard to the previously

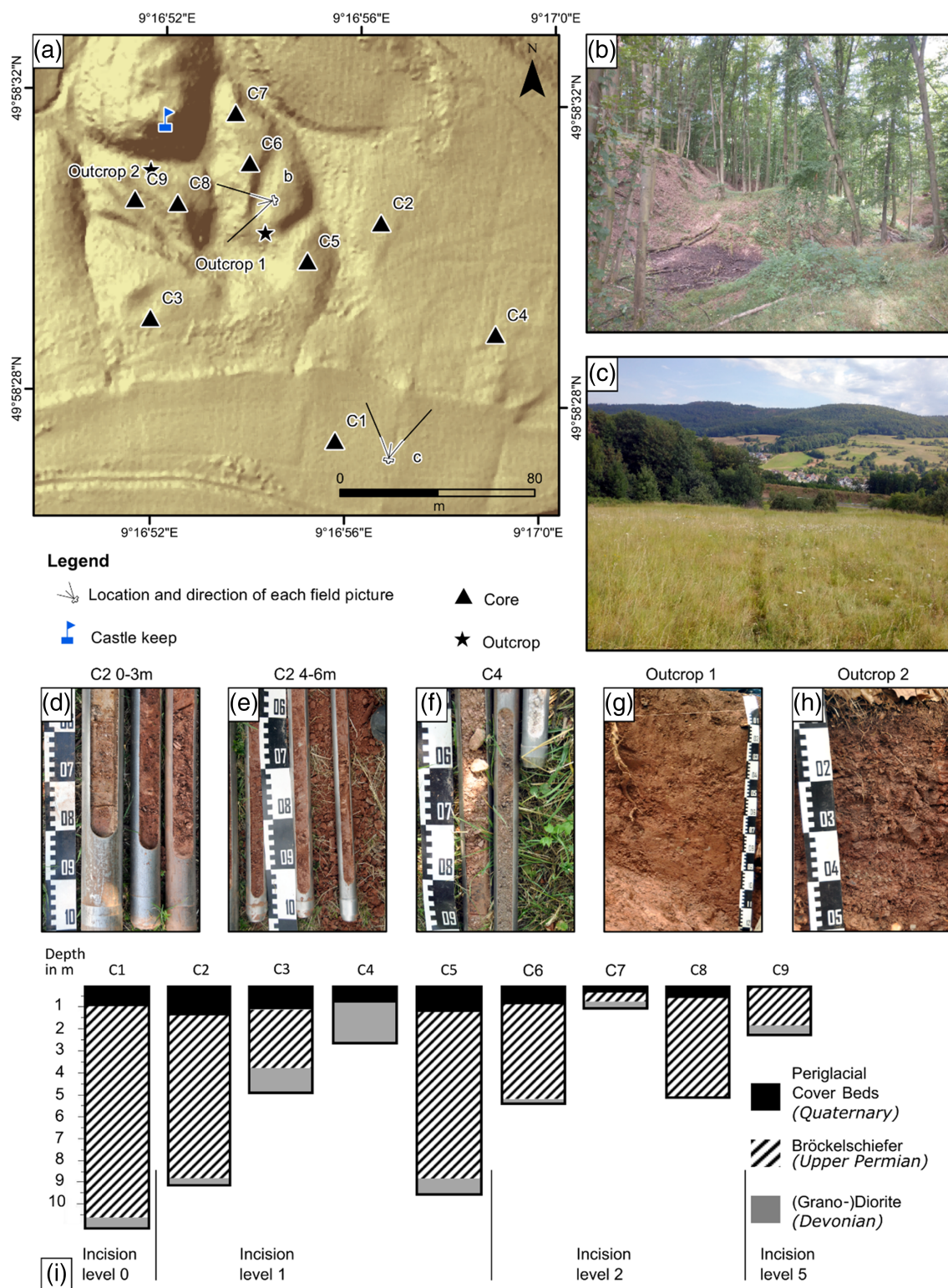


**FIGURE 3** Location of the core sites, photographs of the study area and sediments, and simplified stratigraphy of the cores. (a) Location of the core sites, base map: hillshade from DEM 1 m. (b) Photograph of the scarp (left) and small ridges and valleys (centre and right). (c) Smoothed surface upslope of the rough relief close to the castle. (d–f) Photographs of selected sediment samples: (d) Core C2 0–3 m: Diorite-bearing PCB-layers on top of the Bröckelschiefer; (e) Core C2 3–6 m: intercalated layers of Bröckelschiefer with varying weathering status and colour; (f) Core C4: sample of (Grano-)Diorite saprolite. (g) Outcrop 1: outcropping Bröckelschiefer. (h) Outcrop 2: developed PCBs on top of the eroded (Grano-)Diorite surface. (i) Stratigraphy of the cores C1–C9 sorted after the level of incision (see also Figure 4) [Color figure can be viewed at [wileyonlinelibrary.com](http://wileyonlinelibrary.com)]

described rough relief in the castle's surroundings, two low ridges can be recognized south of the keep (Figure 4a,b). East of these is another, larger ridge that appears rather dissected. It is not mapped as a single unit but is divided into three segments extending from the southeast

in a northwesterly direction to the castle hill, with a total length of nearly 100 m and a height of about 10 m. Two depressions separating the individual ridge segments can be associated with an older drainage pattern eroded in the course of ongoing incision. Episodic streams of

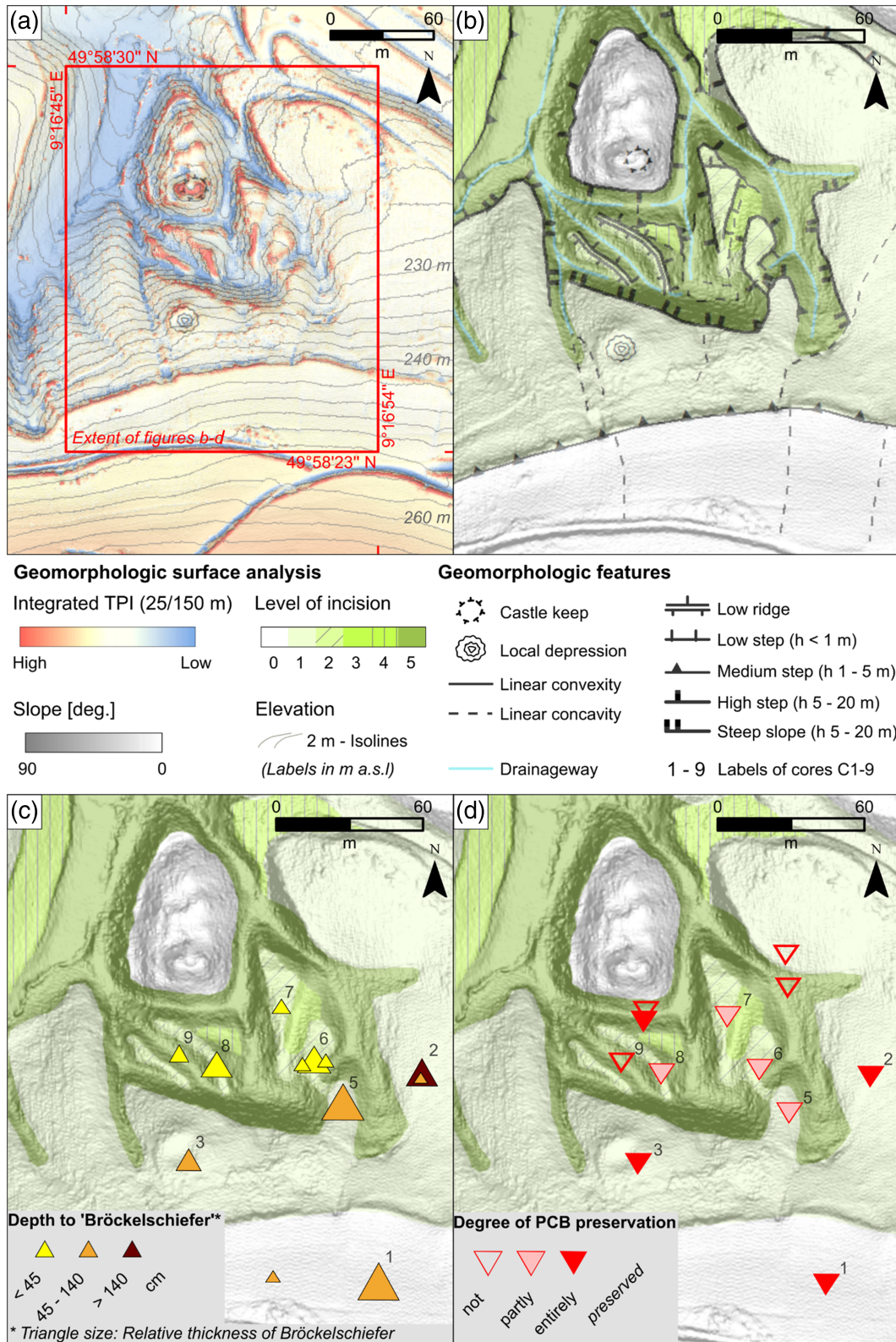


**FIGURE 4** Geomorphological surface analysis and features with stratigraphical data overlay. (a) Integrated view of the 25/150 m TPI highlights steps and ridges at the study site. Red quadrangle marks the map extent of (b) to (d). (b) 'Levels of incision' with associated geomorphological features describing the classified geomorphological properties of the designated levels. (c) Depth and thickness of the Bröckelschiefer as measured in cores and prospection pits at the marked localities. The thickness is directly taken from the extent of the Bröckelschiefer from its upper boundary below the soil or PCB cover, down to the (Grano-)Diorite as the lower boundary. (d) Classes of 'degree of PCB preservation' derived from diagnostic properties observed in cores and prospection pits at the marked localities [Color figure can be viewed at [wileyonlinelibrary.com](http://wileyonlinelibrary.com)]

the recent drainage pattern surround the ridge. In their vicinity, small erosional landforms were also mapped, such as a terrace remnant adjoining the ridges to the north.

A total of six levels of incision could be identified during the geomorphological analyses, which are characterized by the structure and morphometry of their distinct landforms, drainage patterns and

slopes. In the following, all mapped landforms as well as type and thickness of observed stratigraphical layers will be spatially related to these levels (Figure 4b–d).

Incision level 0 is the ‘baseline level’ of the hillslope, which has not been significantly altered by erosion. It includes the gentle surface of the upper slope and the top of the castle site. The north-dipping hillslope south of the castle is extensively used and features several agricultural terraces of unknown age. At this level, the (Grano-)Diorite only starts at a depth of 10.7 m and the Bröckelschiefer has the greatest thickness. The latter is covered by rather thick soils in fully preserved PCBs (cf., core C1; Figures 3i and 4c,d).

Incision level 1 is covered by orchard meadows in the easternmost part of the study area, which are characterized by relatively gentle slopes and low surface roughness. Below the medium terrain step separating level 0 from level 1, the slopes already steepen and the surface roughness is slightly increased compared to level 0. Steep slopes, including a 15 m high scarp in the central study area, characterize the border to level 2 (Figure 4b). The thickness of the Bröckelschiefer is not decreased significantly compared to level 0, but the thickness of the overlying PCBs is considerably increased in some localities (cf., cores C2 and C5) and mostly completely preserved (cf., cores C2 and C3; Figures 3i and 4c,d).

Incision level 2 contains the lower ridges and the lower segments of the main ridge. Steps up to 5 m delimit these landforms as a result of fluvial incision processes. Within this level, the thickness of the Bröckelschiefer decreases downslope, covered by shallow PCBs that are only partially preserved (cf., cores C6, C7 and C8; Figures 3i and 4c,d). In contrast to all other profiles examined in the study area, no Bröckelschiefer was found in core C4 (Figure 3i).

Incision level 3 is represented by a saucer-shaped drainageway separating the two lower segments of the main ridge. It is the remnant of an older drainage pattern that has been largely eroded by more recent incision phases and occurs only sporadically.

Incision level 4 describes a recent to sub-recent erosional terrace level, witnessing the surface of a lower and older drainage level at about 2 m above the recent drainage paths.

Incision level 5 represents the recent drainage system, with varying slopes and drainage activity. At this level the Bröckelschiefer is almost completely eroded and PCBs have only survived on some slopes (cf., core C9; Figures 3i and 4c,d).

### 4.3 | Electrical resistivity tomography (ERT)

In this study, five partly overlapping ERT depth sections are presented, running roughly in south–north and west–east directions through the surroundings of the castle keep. The ERT profiles E1 and E2 are located southeast of the rough relief and display geophysical information of the incision levels 0 and 1. Cores C1, C2 and C4 are located along these ERT measurements and provide the ground truth information. ERT profiles E3, E4 and E5 are located within the rough terrain. These overlap with a variety of incision levels and can be linked with cores C5–C9. The results of the ERT measurements are displayed together with the locations of the core sites and the simplified core stratigraphies in Figure 5.

Overall, the geophysical and stratigraphical data show that the different lithological units of the study area can be assigned to different resistivity ranges. While the claystone of the Bröckelschiefer

can be associated with low resistivity values of 10 to 100  $\Omega\text{m}$ , the (Grano-)Diorite shows electric resistivity values  $> 300 \Omega\text{m}$ . Intermediate resistivity values often occur at the transition between these two lithological units and are probably related to different rock weathering grades. In addition, intermediate resistivity values occur in the surface layers, where they can often be associated with PCBs.

ERT profile E1 shows a two-layer structure with a sharp contrast (Figure 5a). In the northern and southern profile parts, low resistivity values (10–100  $\Omega\text{m}$ ) occur, which can be associated with the claystone of the Bröckelschiefer. Distinguished by a sharp vertical border, the resistivity values increase to more than 350  $\Omega\text{m}$  in the central part of the profile, which is probably related to the presence of (Grano-)Diorite.

In ERT profile E2, a diagonal resistivity change divides the profile into two sections (Figure 5b). The south-eastern part shows resistivity values between 100 and 170  $\Omega\text{m}$ ; the north-western part displays resistivity values below 70  $\Omega\text{m}$ . Combined with the stratigraphic information of cores C2 and C4, the higher values can be associated with the (Grano-)Diorite and the lower ones with the claystone of the Bröckelschiefer.

The ERT profile E3 is located along a ridge, passing incision levels 1, 2 and 3 (Figure 5c). The ERT depth section shows a two-layer composition. At the top, decreasing northwards, a low resistive layer (10–50  $\Omega\text{m}$ ) can be associated with the claystone of the Bröckelschiefer. The higher resistivity values (150–450  $\Omega\text{m}$ ) of the basal layer can probably be explained by the occurrence of (Grano-)Diorite. Therefore, the combination of ERT profile E3 and the cores C5, C6 and C7 shows the downslope decrease of Bröckelschiefer thickness from about 9 to less than 1 m. Close to the surface, lenses of intermediate resistivity values ( $\sim 150 \Omega\text{m}$ ) occur, which can be associated with the PCBs. However, due to their varying thickness and the low resolution of the ERT at the surface, these cannot be resolved throughout the profile.

ERT profile E4, which passes a steep slope in the south, is mainly assigned to the incision levels 1 and 5 and the depth section shows a two- to three-layer composition (Figure 5d). In the intermediate part of the profile there is a low-resistive layer (10–50  $\Omega\text{m}$ ) at the top, which probably consists of Bröckelschiefer and has a maximum thickness of about 10 m. Higher resistivity values ( $\sim 300\text{--}400 \Omega\text{m}$ ) occur in the southern profile part as well as at the bottom layer, which can be associated with (Grano-)Diorite.

ERT profile E5 intersects almost all incision levels (Figure 5e) and the depth section displays two layers. Higher resistivity values (150–800  $\Omega\text{m}$ ) of the basal layer indicate the occurrence of (Grano-)Diorite, while the uppermost, low-resistive layer (10–50  $\Omega\text{m}$ ) is of varying size and corresponds to Bröckelschiefer. In the western part of the profile, (Grano-)Diorite occurs on the surface.

## 5 | DISCUSSION

### 5.1 | Integration of electrical resistivity tomography (ERT) data and stratigraphical fieldwork

The comparison of the ERT data with the stratigraphical information from the cores allowed valid resistivity values for the described lithological units to be derived, with values  $> 300 \Omega\text{m}$  for the (Grano-)Diorite and values of 10 to 100  $\Omega\text{m}$  for the Bröckelschiefer. Remarkably, the values for the (Grano-)Diorite are inconsistent with values from the literature, which typically give values 10 times higher than



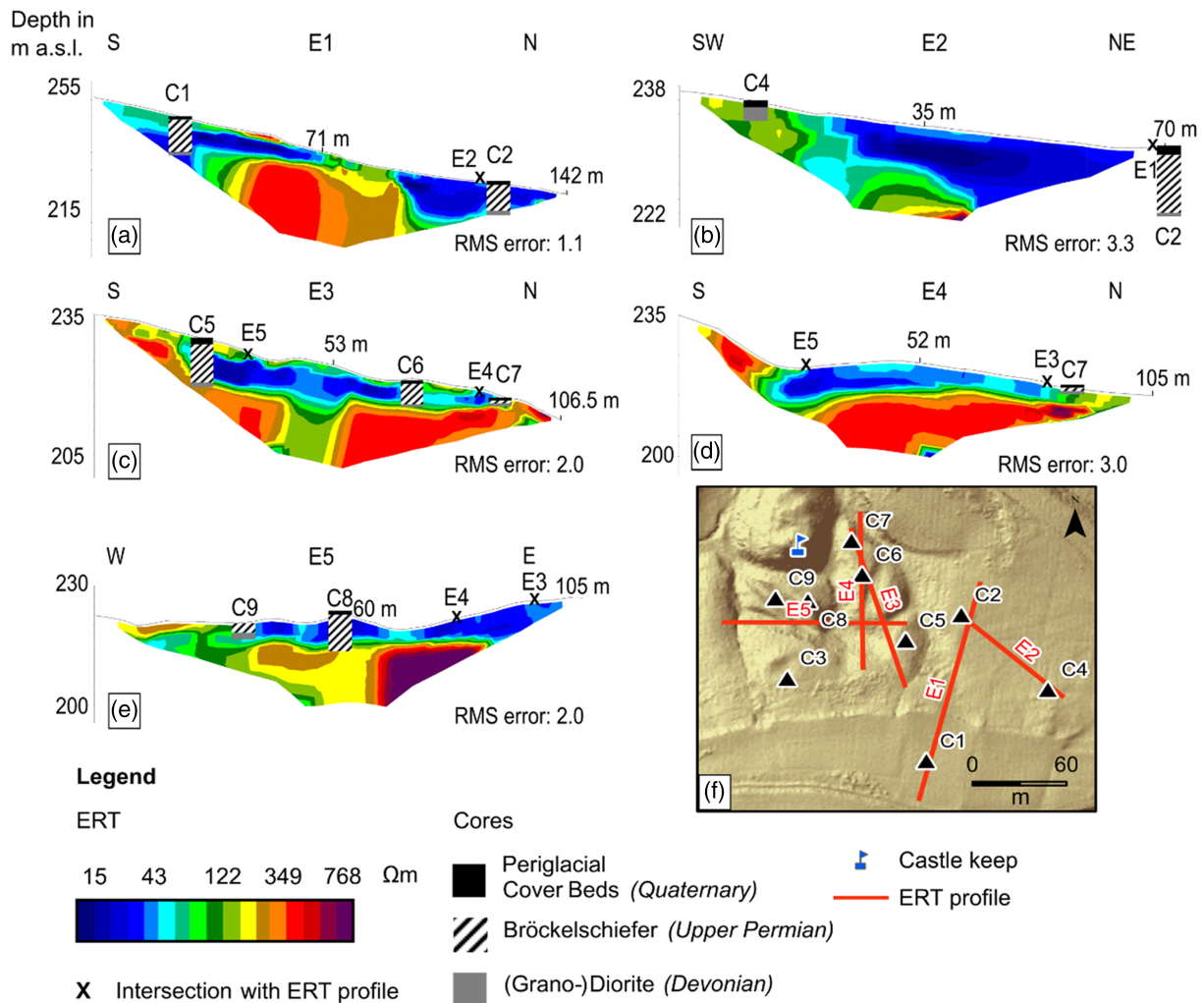


**FIGURE 5** Depth sections of electrical resistivity tomography (ERT) measurements in the surroundings of the castle keep together with the locations and stratigraphy of relevant coring sites. (a) ERT profile E1; (b) ERT profile E2; (c) ERT profile E3; (d) ERT profile E4; (e) ERT profile E5; (f) locations of the ERT profiles E1–E5 and coring sites. Basemap: hillshade calculated from DEM 1 m [Color figure can be viewed at [wileyonlinelibrary.com](http://wileyonlinelibrary.com)]

those observed (Reynolds, 2011). One explanation for this discrepancy is probably the high degree of intensive chemical weathering and fracturing of the rocks. Furthermore, the great number of local springs within the study area indicates a high water content of the weathered (Grano-)Diorite. Both weathering and moisture changes can significantly reduce the resistivity of rock material (Reynolds, 2011).

However, the ERT measurements were not sensitive enough to detect the thin layers of the PCBs consistently in all profiles. This is probably due to the large electrode spacing (1.5–3 m) of the measurements (Reynolds, 2011). These were chosen in this study to reliably map the Bröckelschiefer–(Grano-)Diorite boundary assumed at about 10 m depth by previous investigations. The stratigraphic results of the cores and trenches therefore provide the more reliable data on PCB distribution in the study area.

## 5.2 | Spatial correlation of lithological units and landforms

The spatial distribution of the lithological units and their correlation with the landforms indicate a close relationship of landform genesis and type and origin of the subsurface materials.

ERT profiles E1 and E2 indicate a high thickness of Bröckelschiefer around several faults in the area (cf., Figures 5a,b and 7). Hence, the vertical change in resistivity within ERT profile E2 obviously indicates a fault-related anomaly affecting the bedrock distribution of the shallow subsurface. A potential localization of the faulting can also be derived from ERT profile E1 where (Grano-)Diorite only occurs in the central part. Here signs of faulting appear with steep vertical steps separating the Bröckelschiefer from the (Grano-)Diorite. A subsurface vertical gradient is also observed in ERT profile E3, the extent of which corresponds directly to the course of the prominent steep slope (Figure 6). Therefore, the relocation of the Bröckelschiefer, forming the relief south of the castle, seems spatially dependent on both the steep slope and a fault-system, which was partly mapped by Weinelt (1962). The scarp of the fault is best visible in ERT profile E4 due to the occurrence of (Grano-)Diorite in the south. ERT profile E5 shows the decreasing thickness of the Bröckelschiefer downslope. Moreover, the small ridges are made of Bröckelschiefer. The subsurface of the valleys shows that erosion in this area only affects the Bröckelschiefer; the (Grano-)Diorite is not incised (Figure 6).

Overall, the combined geoelectrical and stratigraphical data show that the rough relief south of the castle hill was formed across the Bröckelschiefer overlying the (Grano-)Diorite. This results in a greater

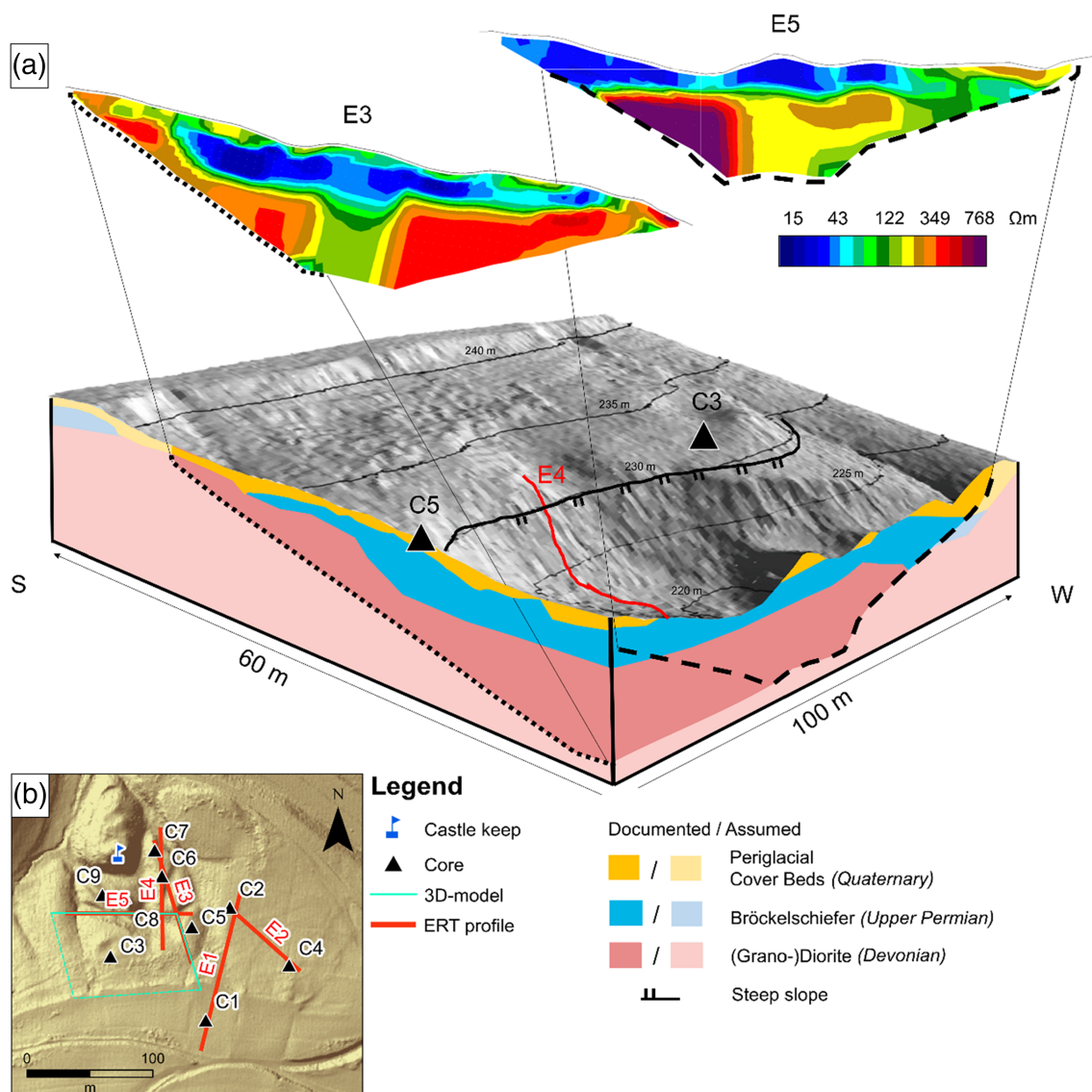


**FIGURE 6** (a) Pseudo three-dimensional visualization of a geological model of the area south of the castle hill. (b) Locations of the ERT profiles and core sites. Basemap: hillshade calculated from DEM 1 m [Color figure can be viewed at [wileyonlinelibrary.com](http://wileyonlinelibrary.com)]

downslope extension of the Bröckelschiefer than Weinelt (1962) had previously assumed (Figure 7).

### 5.3 | Landscape evolution

The particular spatial configuration of the crystalline Devonian (Grano-)Diorite and the Late Permian sedimentary rocks of the Bröckelschiefer is the result of specific geomorphological structures and processes, which form the basis for a hypothetical morphogenetic model. This model starts in the Eocene with undifferentiated planation and the onset of faulting activity in the Oligocene. Subsequently the model is divided into two possible scenarios during the phase of restrictive planation, which took place from the onset of the Lower Miocene as described in regional studies (Figure 8; Boldt, 1998; Jung, 2006). (1) The first scenario considers a theory proposed by Weinelt (1962). When mapping the Bröckelschiefer formation north of Waldaschaff, he observed that the bottom layers strike in the opposite direction to the overall dip of the Mesozoic Buntsandstein formations covering the Bröckelschiefer in the wider study area. This

notable divergence makes Early Miocene subsidence of the local fault blocks likely (Weinelt, 1962). The implied faulting activity then probably weakened the structure and texture of the bedrock, making it locally susceptible to intense Miocene weathering (cf., Jung, 2006; Okrusch et al., 2011).

(2) However, as evidence of sliding processes and intensive solifluction were observed in the study area, the occurrence of Bröckelschiefer in local depressions could also be the result of mass movements during one or more phases. According to this, the Bröckelschiefer units are deposits that have moved downslope by slipping and sliding processes and are now covering the (Grano-)Diorite (Figure 8b, second phase). This scenario is supported by a study by Lorenz et al. (2010) who described claystone layers with traces of sediment movement in an outcrop only a few hundred metres from the castle site.

Either way, the Buntsandstein cover was mostly eroded during the Miocene, whereas the Bröckelschiefer was preserved in varying thickness depending on its relief position. Exposed to deep chemical dissolution, the weathering residues remained in the form of saprolite (Figure 8, third phase). In the course of the Pliocene and Pleistocene, erosion and fluvial incision exceeded chemical weathering and

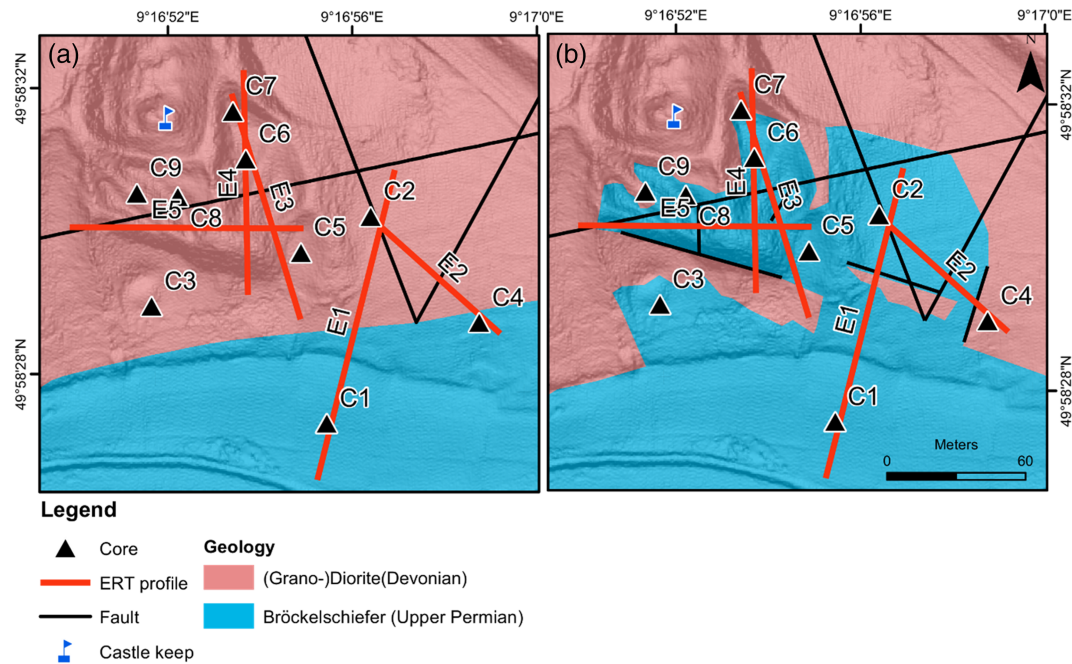


**FIGURE 7** Geological map of the study area. (a) Geological situation after Weinelt (1962). (b) Reinterpreted geological situation based on the field data of this study [Color figure can be viewed at [wileyonlinelibrary.com](https://onlinelibrary.wiley.com)]

denudation. This led to a more accentuated relief and altered morphodynamics, including the increased occurrence of solifluction and sliding processes during the Late Pleistocene (Figure 8, fourth phase).

Due to the lack of dating possibilities, the timing of the earlier-mentioned processes remains unclear. However, a simple chronological order of the events can at least be established. The main sliding, faulting and erosional activities must have taken place before the formation of the PCBs, as seen by their widespread distribution and good preservation within the study area. Furthermore, the PCBs' inclination is often adjusted to a former drainage system, as observed for instance at the incision levels 3 and 4 (cf., Figure 4d). Here, the PCBs cover the weathered surface of the (Grano-)Diorite, which accordingly has probably been evenly eroded and smoothed by effective solifluction processes. Taken overall, this suggests effective (Grano-)Diorite erosion even before the incision reached its recent level during the Holocene.

The youngest sediments were observed in the castle's neck trench. Here, the castle builders over-deepened the drainageway directly south of the castle hill with a neck trench in order to strengthen the fortifications. In the course of the castle's destruction in 1266 CE, the castle walls collapsed and entirely refilled the neck trench (Rosmanitz & Bachmann, 2017). The debris still buries the thalweg level of the drainage system and colluvial layers cover the PCBs of the adjacent slopes. The late- and post-medieval erosion thus did not reach the bottom of this former valley.

#### 5.4 | Potential locational factors of Wahlmich Castle

The study results show that Wahlmich Castle was placed on top of a small isolated hard-rock hill made of crystalline (Grano-)Diorite in a midslope to footslope position, whereas the surrounding terrain

consists of claystone of the Bröckelschiefer formation or intensively weathered (Grano-)Diorite. This circumstance was apparently known in the Middle Ages and was intentionally used for the excavation of a neck trench at the foot of the castle hill. Apart from this, however, no outer bailey or evidence for other anthropogenic building activities were found in the castle surroundings. The rough relief and the lithology that the medieval castle builders faced were obviously prone to erosion and therefore people evidently avoided intensive land use and building activities on such slopes and ridges. Overall, the specific geomorphological and geological situation of Wahlmich Castle characterized by faulting, mass movement and fragmentation is unique within the Spessart and the site properties substantially diverge from those of other castles in the region (Rosmanitz et al., 2019a). Despite the natural limitations for land use and the resulting low attractiveness of the site for land ownership, however, there were obviously locational factors that motivated the construction of a castle at this location.

One possible reason might have been the control of traffic routes. Several sunken roads exist near Wahlmich Castle that once connected the site and the Aschaff River valley with the important medieval traffic routes of several European trading cities (Himmelsbach, 2014; Landau, 1958). The individual roads thereby often follow the local land-use boundaries or lie far beyond the former farmland (Himmelsbach, 2005, 2014). Another economic reason for the location of Wahlmich Castle could possibly be the quarrying of iron ore deposits. There is still visible evidence of earlier quarrying activities in the immediate vicinity, even though documentary records of these efforts only exist from the 18th century onwards (Lorenz et al., 2010).

Moreover, the local political power structure may have played an important role in the choice of location. The political environment of the time was determined by the struggle for political and economic supremacy between the rival clerical and secular lords. The secular Counts of Rieneck, who wanted to demonstrate their claim to the Aschaff River valley, are considered to be the builders of Wahlmich Castle (Gröber & Karlinger, 1916; Rosmanitz et al., 2019b). This was

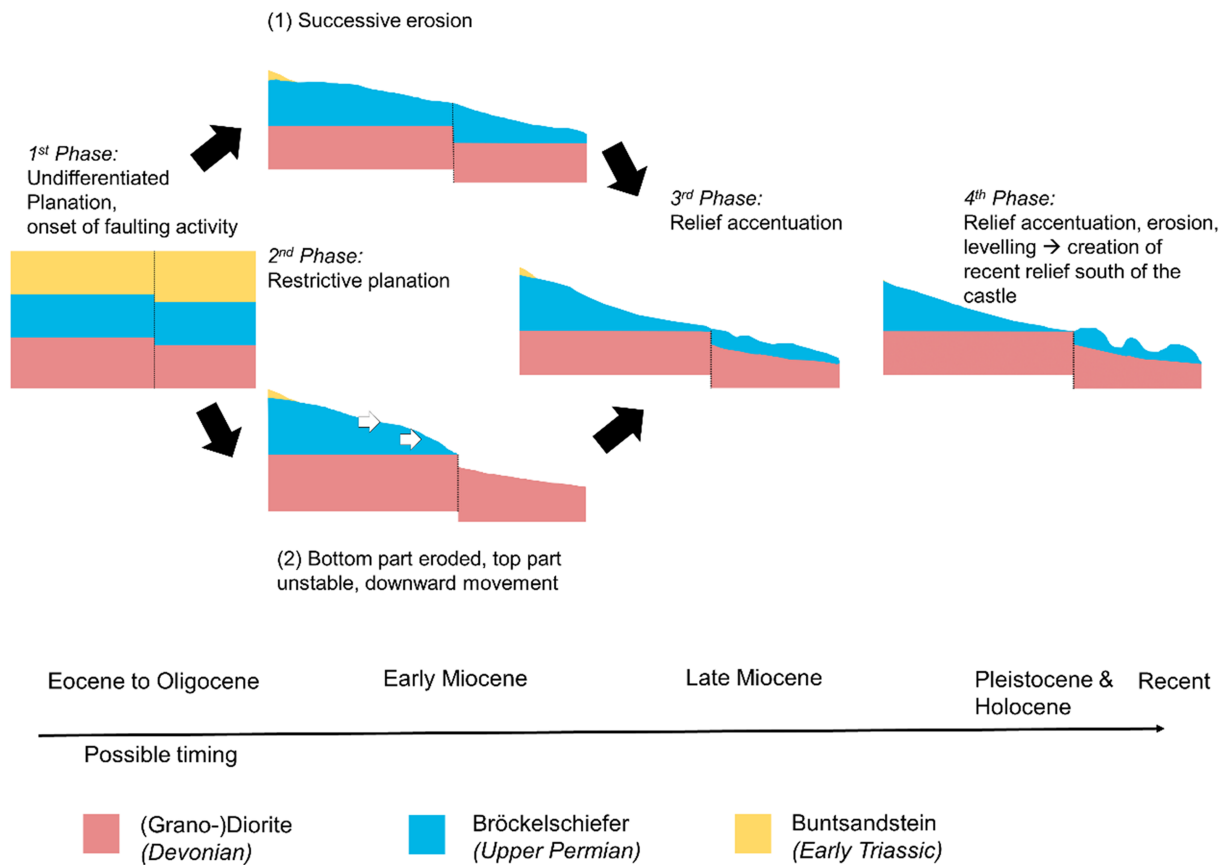


**FIGURE 8** Conceptual models of the local landscape evolution depicting two pathways (1 and 2) that may have led to the formation of the current geological situation in the study area [Color figure can be viewed at [wileyonlinelibrary.com](https://onlinelibrary.wiley.com)]

certainly a challenge to the Bishops of Mainz, whose residence town of Aschaffenburg was only a few kilometres away. Their territorial claim to the Aschaff River valley is expressed in numerous contemporary documents that regulate the bishop's forest ban in the Spessart and an associated forest administration in the immediate vicinity of Wahlmich Castle (Büttner, 1961; Franz, 2020). The claim to ownership of this area by the Counts of Rieneck could thus provide an explanation for the rather isolated location of Wahlmich Castle.

Overall, it seems that the economic situation combined with rivalry between different elites in the Aschaff River valley led to the castle being built in this unspectacular, almost remote and strategically less valuable mid-slope geomorphological position. This indicates that castle sites can also be expected in agriculturally unfavourable regions and/or at unique geomorphological sites, where other economic and political factors must have favoured the choice of location, even if they are difficult to prove historically.

## 6 | CONCLUSION

While anthropogenic influence on a landscape has often been discussed in science and proven in various case studies (e.g., Brown et al., 2017; Bork, 2020; Henselowsky et al., 2021), the example of the surrounding of Wahlmich Castle shows a different picture. Today, easily erodible ridges and valleys of weathered Bröckelschiefer form a rough landscape around the castle hill, which stands in strong contrast to the mostly gentle hills of the Spessart low mountain range. The analysis of sediment and geophysical data showed that regional

faulting caused subsidence and subsequent fragmentation of the sediment body, which triggered the weathering and dissection of the surface deposits. The vertical offset caused by the faulting and the increased potential energy could also have triggered sliding and slumping of the Bröckelschiefer. Thus, despite the impression of a landscape that has been highly anthropogenically influenced and apart from building activity at the castle hill, the evidence supporting a natural origin of the relevant forming processes prevails. Accordingly, Wahlmich Castle is an anthropogenic structure built in a natural but exceptional geomorphological and geological setting.

In a supra-regional context, the location of the castle site close to the central Spessart and the cuesta scarp is not typical. Most of the known castles are located in dissection areas and in regions overlain by comparably young, fluvial deposits. The castles commonly provided access to the resources of the Spessart, such as beech wood for glass production and waterpower. Moreover, access to and control over important medieval traffic routes and potential for representing authority were important factors determining the locations of castle construction within the Spessart. As a special case, Wahlmich Castle was located in an area where tectonically induced cuesta scarp erosion made effective land use impossible. Thus, rival claims of control and ownership over the Aschaff River valley in the context of a political and economic feud probably led to the construction of the castle at this location. Strategically unfavourable castle sites are also known from other geomorphological domains, for example, in the Kirschgraben valley on an alluvial fan (Larsen et al., 2013) or in the case of Hauenstein Castle, on a riverbank, which emerged from a medieval water mill (Rosmanitz et al., 2019a). The conservation

conditions in such areas can be considered comparatively poor. It seems that focusing on geomorphologically rare and challenging locations may lead to a better understanding of castle siting in the future, and it may help to find more castle sites in comparable geomorphological and geological settings.

This study also demonstrates the importance of comprehensive geomorphological investigations for the identification and evaluation of castle sites in terms of factors influencing site selection. Furthermore, the thorough investigation of multiple interdependent landscape-forming processes also allows for a discussion of the constraints resulting from competing land-use pressures in particular landscapes.

## ACKNOWLEDGEMENTS

The authors would like to thank all members of the 'Archäologische Spessartprojekt', especially Harald Rosmanitz, Sabrina Bachmann and Michael Geisslinger, for their archaeological and logistical support and the interdisciplinary discussion of the results. Further acknowledgements go to Wolfgang and Angelika Beyer and their team from the Verein für Heimatpflege Waldaschaff e.V. The authors kindly thank three anonymous reviewers for thoroughly evaluating the manuscript; their valuable comments and suggestions considerably improved earlier versions of this manuscript. The authors also thank Dr Katharine Thomas for proofreading the manuscript.

## CONFLICT OF INTEREST

The authors declare that they have no conflict of interest.

## DATA AVAILABILITY STATEMENT

The data used in this study are available upon request from the authors.

## ORCID

Julian Trappe  <https://orcid.org/0000-0002-7580-9483>

Christian Büdel  <https://orcid.org/0000-0002-3376-1688>

Julia Meister  <https://orcid.org/0000-0003-1385-4112>

Roland Baumhauer  <https://orcid.org/0000-0001-9712-7611>

## REFERENCES

- Ad-hoc Boden. (2005) *Bodenkundliche Kartieranleitung: mit 103 Tabellen und 31 Listen*. 5th edition. Stuttgart: Schweizerbart.
- Bayerisches Landesamt für Digitalisierung, Breitband und Vermessung. (2014) DGM 1m. Augsburg: Bayerisches Landesamt für Umwelt.
- Bayerisches Landesamt für Landwirtschaft. (2019) *AgrarMeteorologie Bayern: Wetterdaten*. Augsburg: Bayerisches Landesamt für Umwelt.
- Bayerisches Landesamt für Umwelt. (2015) *Übersichtsbodenkarte TK25-Blatt 6021 Haibach*. Augsburg: Bayerisches Landesamt für Umwelt.
- Bernatek-Jakiel, A. & Kondracka, M. (2016) Combining geomorphological mapping and near surface geophysics (GPR and ERT) to study piping systems. *Geomorphology*, 274, 193–209. <https://doi.org/10.1016/j.geomorph.2016.09.018>
- Boldt, K. (1998) The model of restrictive planation - an approach towards understanding the rules of landform development in sedimentary rocks of variable resistance. *Zeitschrift für Geomorphologie*, 42(1), 21–37. <https://doi.org/10.1127/zfg/42/1998/21>
- Bork, H.-R. (2020) *Umweltgeschichte Deutschlands*. Berlin, Heidelberg: Springer 10.1007/978-3-662-61132-6.
- Brown, A.G., Tooth, S., Bullard, J.E., Thomas, D.S.G., Chiverrell, R.C., Plater, A.J. et al. (2017) The geomorphology of the Anthropocene: emergence, status and implications. *Earth Surface Processes and Landforms*, 42(1), 71–90. Available from: <https://doi.org/10.1002/esp.3943>
- Büdel, C., Kempf, B., Rüppel, J. & Nelle, O. (2021) *Der Wald im Spessart: Entwicklung des Spessartwaldes*, Spessart. Vol. 1. Achaffenburg: Main Echo.
- Büttner, W. (1961) *Geschichte des Dorfes Waldaschaff und der Pfarrei Keilberg*. Achaffenburg: Paul Pattloch Verlag Achaffenburg.
- Champagnac, J.-D., Valla, P.G. & Herman, F. (2014) Late-Cenozoic relief evolution under evolving climate: A review. *Tectonophysics*, 614, 44–65. <https://doi.org/10.1016/j.tecto.2013.11.037>
- Dahlin, T. & Zhou, B. (2004) A numerical comparison of 2D resistivity imaging with 10 electrode arrays. *Geophysical Prospecting*, 52(5), 379–398. <https://doi.org/10.1111/j.1365-2478.2004.00423.x>
- Ermischer, G. (2019) Der gläserne Wald: Glasproduktion im Spessart. *Bayerische Archäologie*, 4, 36–41.
- Fischer, P., Meurers-Balke, J., Gerlach, R., Bulla, A., Peine, H.-W., Kalis, A.J. et al. (2016) Geoarchaeological and archaeobotanical investigations in the environs of the Holsterburg lowland castle (North Rhine-Westphalia) – evidence of landscape changes and salt-water upwelling. *Zeitschrift für Geomorphologie, Supplementary Issues*, 60(1), 79–92. [https://doi.org/10.1127/zfg\\_suppl/2015/S-00186](https://doi.org/10.1127/zfg_suppl/2015/S-00186)
- Franz, T. (2020) *Geschichte der deutschen Forstverwaltung*. Berlin: Springer Fachmedien: Wiesbaden 10.1007/978-3-658-28658-3.
- Freymann, K. (1991) *Der Metallerzbergbau im Spessart: Ein Beitrag zur Montangeschichte des Spessarts*. Achaffenburg: Geschichts- und Kunstverein Achaffenburg e. V.
- Gröber, K. & Karlinger, G. (1916) *Die Kunstdenkmäler des Königreichs Bayern: Regierungsbezirk Unterfranken & Achaffenburg*. München: Druck und Kommissionsverlag von R. Oldenbourg.
- Guisan, A., Weiss, S.B. & Weiss, A.D. (1999) GLM versus CCA spatial modeling of plant species distribution. *Plant Ecology*, 143(1), 107–122. <https://doi.org/10.1023/A:1009841519580>
- Hasenstein, L., Geschwinder, R. & Bergmann, C. (2019) Relikte mittelalterlicher Eisengewinnung und einer Wüstung bei Steinau an der Straße. *Jahrbuch für Archäologie Und Paläontologie in Hessen*, 2018, 186–188.
- Henselowsky, F., Rölken, J., Kelterbaum, D. & Bubenzer, O. (2021) Anthropogenic relief changes in a long-lasting lignite mining area ('Ville', Germany) derived from historic maps and digital elevation models. *Earth Surface Processes and Landform*, 46(9), 1725–1738. <https://doi.org/10.1002/esp.5103>
- Himmelsbach, G. (2005) *Kurfürstenweg. Spessart: Europäische Kulturwege im Spessart und Odenwald*, p. 99.
- Himmelsbach, G. (2014) Frühneuzeitlicher Viehhandel und Kulturlandschaftsforschung im Spessart. *Bulletin der Polnischen Historischen Mission*, 9(0), 153–173. <https://doi.org/10.12775/BPMH.2014.006>
- Jung, J. (2006) *GIS-gestützte Rekonstruktion der neogenen Reliefentwicklung tektonisch beeinflusster Mittelgebirgslandschaften am Beispiel des Spessarts (NW-Bayern, SE-Hessen)*. Würzburg: Universität Würzburg.
- Käding, K.-C. (1978) Die Grenze Zechstein/Buntsandstein in Hessen, Nordbayern und Baden-Württemberg. *Jahresberichte Und Mitteilungen Des Oberrheinischen Geologischen Vereins*, 60, 233–252. <https://doi.org/10.1127/jmogv/60/1978/233>
- Kampfmann, G. & Krimm, S. (1988) *Verkehrsgeographie und Standorttypologie der Glashütten im Spessart*. Achaffenburg: Geschichts- und Kunstverein Achaffenburg e. V.
- Kaufmann, G. & Romanov, D. (2017) The Jettencave, Southern Harz Mountains, Germany: Geophysical observations and a structural model of a shallow cave in gypsum/anhydrite-bearing rocks. *Geomorphology*, 298, 20–30. <https://doi.org/10.1016/j.geomorph.2017.09.027>
- Kemethmüller, L. (2011) The history of the Castle landscape in the German Spessart. *Concilium Medii Aevi*, 14, 93–99.
- Kleber, A. (1997) Cover-beds as soil parent materials in midlatitude regions. *Catena*, 30(2-3), 197–213. [https://doi.org/10.1016/S0341-8162\(97\)00018-0](https://doi.org/10.1016/S0341-8162(97)00018-0)
- Kleber, A. & Terhorst, B. (2013) *Mid-Latitude Slope Deposits (Cover Beds)*. Oxford: Elsevier Science.

- Kolb, P. & Krenig, E.-G. (1989) *Unterfränkische Geschichte: Von der germanischen Landnahme bis zum hohem Mittelalter*. Würzburg: Echter.
- Lagies, M. (2005) Neue pollenanalytische Forschungen in Spessart und Odenwald – eine Zusammenfassung. *Carolinea*, 63, 113–134.
- Landau, G. (1958) *Beiträge zur Geschichte der alten Heer- und Handelsstraßen in Deutschland*. Kassel: Bärenreiter-Verlag.
- Lange-Athinodorou, E., El-Raouf, A.A., Ullmann, T., Trappe, J., Meister, J. & Baumhauer, R. (2019) The sacred canals of the Temple of Bastet at Bubastis (Egypt): New findings from geomorphological investigations and Electrical Resistivity Tomography (ERT). *Journal of Archaeological Science: Reports*, 26, 101910. <https://doi.org/10.1016/j.jasrep.2019.101910>
- Larsen, A., Bork, H.-R., Fuelling, A., Fuchs, M. & Larsen, J. (2013) The processes and timing of sediment delivery from headwaters to the trunk stream of a Central European mountain gully catchment. *Geomorphology*, 201(1), 215–226. <https://doi.org/10.1016/j.geomorph.2013.06.022>
- Leser, H. & Stäblein, G. (1985) *Geomorphologische Kartieranleitung: Richtlinien zur Herstellung geomorphologischer Karten 1:25.000*. Berlin: Inst. für Physische Geographie d. Freien Univ. Berlin.
- Lorenz, J., Okrusch, M., Geyer, G., Jung, J., Himmelsbach, G. & Dietl, C. (2010) *Spessartsteine: Spessartin, Spessartit und Buntsandstein - eine umfassende Geologie und Mineralogie des Spessarts; geographische, geologische, petrographische, mineralogische und bergbaukundliche Einsichten in ein deutsches Mittelgebirge*. Karlstein am Main: Lorenz.
- Meschede, M. (2019) *Geologie Deutschland: Ein prozessorientierter Ansatz*, 2nd edition. Berlin: Springer Spektrum.
- Mueller, S. (2011) *New insights about Pleistocene periglacial slope deposits and pedogenesis in the Hessian Spessart Mountains*. Dissertation, 2011. Frankfurt am Main: Univ. Frankfurt am Main.
- Mueller, S. & Thiemeyer, H. (2014) Formation and transformation of Pleistocene periglacial slope deposits in the Spessart Mountains (Hesse, Germany). *Zeitschrift für Geomorphologie*, 58(3), 91–113. <https://doi.org/10.1127/0372-8854/2014/S-00157>
- Murawski, H. (1965) Der Spessart als Teilgebiet der Mitteldeutschen Schwelle. *Geologische Rundschau*, 54(2), 835–852. <https://doi.org/10.1007/BF01820758>
- Okrusch, M., Geyer, G. & Lorenz, J. (2011) *Sammlung geologischer Führer Band 106: Spessart: Geologische Entwicklung und Struktur, Gesteine und Minerale*. Stuttgart: Gebrüder Bornträger.
- Reynolds, J.M. (2011) *An introduction to applied and environmental geophysics*. 2nd edition. Chichester: Wiley-Blackwell.
- Rosmanitz, H. (2011) The castle project in the Spessart – scientists and volunteers explore a cultural landscape. *Concilium Medii Aevi*, 14, 101–120.
- Rosmanitz, H. & Bachmann, S. (2017) Waldaschaff, Lkr. Aschaffenburg, Burg Wahlmich, Archäologische Untersuchung: Mai - August 2016. Bayerisches Landesamt für Denkmalpflege; excavation report: Maßnahmen-Nr. M-2016-799-1\_0.
- Rosmanitz, H., Bachmann, S. & Geißlinger, M. (2019a) Krombach, Lkr. Aschaffenburg, Burg Hauenstein: Archäologische Untersuchung, August - November 2017. Bayerisches Landesamt für Denkmalpflege; excavation report: Maßnahmen-Nr. M-2017-1232-1\_0.
- Rosmanitz, H., Bachmann, S. & Geißlinger, M. (2019b) Waldaschaff, Lkr. Aschaffenburg, Burg Wahlmich. Bayerisches Landesamt für Denkmalpflege; excavation report: Maßnahmen-Nr. M-2018-871-1\_0.
- Ruf, T. (1984) *Die Grafen von Rieneck Genealogie und Territorienbildung: II. Herkunftstheorien und Systematik der Territorienbildung*. Würzburg: Freunde Mainfränkischer Kunst und Geschichte e.V.
- Ruf, T. (2019) Zur Geschichte einiger Spessartburgen im 12. und 13. Jahrhundert. *Aschaffener Jahrbuch für Geschichte, Landeskunde und Kunst im Untermaingebiet*, 33, 9–93.
- Sass, O., Bell, R. & Glade, T. (2008) Comparison of GPR, 2D-resistivity and traditional techniques for the subsurface exploration of the Öschingen landslide, Swabian Alb (Germany). *Geomorphology*, 93(1–2), 89–103. <https://doi.org/10.1016/j.geomorph.2006.12.019>
- Schäfer, R. (2000) *Die Herren von Eppstein*. Wiesbaden: Historische Kommission Nassau.
- Schecher, O. (1969) *Die Grafen von Rieneck: Zur Geschichte eines mittelalterlichen Hochadelsgeschlechts in Franken*. Lohr am Main: Schriften des Geschichtsvereins.
- Scheinpflug, R. (1992) *Main-Spessart-Geologie: mit 7 Tabellen*. Lohr am Main: Mineralogisch-Paläontologische Privatsammlung Scheinpflug.
- Shishkina, Y.V., Garankina, E.V., Belyaev, V.R., Shorkunov, I.G., Andreev, P. V., Bondar, A.I. et al. (2019) Postglacial incision-infill cycles at the Borisoglebsk Upland: Correlations between interfluvial headwaters and fluvial network. *International Soil and Water Conservation Research*, 7(2), 184–195. <https://doi.org/10.1016/j.iswcr.2019.02.001>
- Siart, C., Forbriger, M. & Bubenzer, O. (Eds.) (2018) *Digital geoarchaeology: New techniques for interdisciplinary human-environmental research*. Cham: Springer 10.1007/978-3-319-25316-9.
- Siart, C., Hecht, S., Holzhauser, I., Altherr, R., Meyer, H.P., Schuhkraft, G. et al. (2010) Karst depressions as geoarchaeological archives: The palaeoenvironmental reconstruction of Zominthos (Central Crete), based on geophysical prospection, sedimentological investigations and GIS. *Quaternary International*, 216(1–2), 75–92. <https://doi.org/10.1016/j.quaint.2009.06.020>
- Telford, W.M., Geldart, L.P. & Sheriff, R.E. (1990) *Applied Geophysics*. Cambridge: Cambridge University Press. <https://doi.org/10.1017/CBO9781139167932>
- Trappe, J. & Kneisel, C. (2019) Geophysical and sedimentological investigations of peatlands for the assessment of lithology and subsurface water pathways. *Geoscience*, 9(3), 118. <https://doi.org/10.3390/geosciences9030118>
- Wamser, L. (1979) *Glashütten im Spessart: Gewinne und Verluste*. München: Ausgrabungsnotizen aus Bayern.
- Wamser, L. (1982) Neue Ausgrabungen mittelalterlicher Spessart-Glashütten bei Schöllkrippen, Landkreis Aschaffenburg, Unterfranken. *Das Archäologische Jahr in Bayern*, 2, 188–189.
- Wedepohl, K.H. (2003) *Glas in Antike und Mittelalter: Geschichte eines Werkstoffs*. Stuttgart: E. Schweizerbart'sche Verlagsbuchhandlung.
- Weinelt, W. (1962) *Geologischen Karte von Bayern 1:25 000. Blatt Nr. 6021 Haibach: mit Erläuterungen*. München: Bayerisches Geologisches Landesamt.
- Weiss, A. (2001) Topographic Position and Landforms Analysis, ESRI user conference, 2001.
- Zerbe, S. (1997) Stellt die potentielle natürliche Vegetation (PNV) eine sinnvolle Zielvorstellung für den naturnahen Waldbau dar? *Forstwissenschaftliches Centralblatt*, 116(1–6), 1–15. <https://doi.org/10.1007/BF02766877>

**How to cite this article:** Trappe, J., Büdel, C., Meister, J. & Baumhauer, R. (2022) Combining geophysical and geomorphological data to reconstruct the development of relief of a medieval castle site in the Spessart low mountain range, Germany. *Earth Surface Processes and Landforms*, 47(1), 228–241. Available from: <https://doi.org/10.1002/esp.5242>